Proceedings of the 9th U.S. National and 10th Canadian Conference on Earthquake Engineering
Compte Rendu de la 9ième Conférence Nationale Américaine et
10ième Conférence Canadienne de Génie Parasismique
July 25-29, 2010, Toronto, Ontario, Canada • Paper No 229

BEHAVIOR OF REINFORCED CONCRETE CORNER BEAM-COLUMN JOINTS WITHOUT TRANSVERSE REINFORCEMENT

Sangjoon Park[1] and Khalid M. Mosalam[2]

ABSTRACT

Four full-scale reinforced concrete (RC) corner beam-column joints without transverse reinforcement in the joint region were constructed with floor slabs between two orthogonal beams to assess the vulnerability of old RC buildings. The specimens were designed considering two parameters: (1) joint aspect ratio expressed as the ratio of beam depth to column depth and (2) the amount of longitudinal beam reinforcement. To focus on a corner beam-column joint shear failure, beams and column were designed according to the strong column-weak beam scheme. This paper reports the experimental results of specimen SP1 having low beam reinforcement ratio (0.67%) with low joint aspect ratio (1:1), which was tested first under quasi-static cyclic uni-directional loading alternating between the two orthogonal beam directions. During testing, the column axial load varied linearly with the beam shear force such that the fluctuation of the column axial load due to overturning moment was simulated. Specimen SP1 was governed by joint shear failure following beam yielding. The obtained shear strength of SP1 from the test results is compared with the predictions from newly developed beam-column joint strength models, which are briefly presented in this paper.

Introduction

Reinforced concrete (RC) buildings designed during the 1960s and 1970s still widely exist in the western US and in other seismically active regions worldwide. The beam-column joints of these buildings are vulnerable to earthquake loads due to insufficient shear reinforcement in the joint region. To estimate the shear strength of RC beam-column joints without transverse reinforcement (denoted as “unreinforced”), a large number of tests have been conducted with different joint geometries, beam reinforcement ratios and anchorage details, and column axial load ratios in US , Japan, New Zealand, United Kingdom and other places. Tests from literature showed that ASCE/SEI 41-06 may underestimate the shear strength of unreinforced exterior joints. However, the majority of tests from literature were conducted with two dimensional (2D) exterior joints under constant column axial loading during tests. In this study, four full-scale unreinforced corner beam-column joints were constructed with floor slabs

[1] Ph.D. Candidate, Department of Civil and Environmental Engineering, University of California, Berkeley, CA 94720-1710, Email: sangjoon@berkeley.edu.
[2] Professor and Vice Chair, 733 Davis Hall, Department of Civil and Environmental Engineering, University of California, Berkeley, CA 94720-1710, Email: mosalam@ce.berkeley.edu.

between two orthogonal beams and recently one of these four specimens was tested with quasi-static cyclic uni-directional loading alternating between the two orthogonal beam directions. In parallel with the experimental study, new joint shear strength models were developed by semi-empirical and analytical approaches (Park and Mosalam, 2009). The accuracy of the proposed joint shear strength models is investigated in this paper by comparisons between the analytical predictions and the test results.

Experimental Program

Specimen Configuration and Test Matrix

The experimental program consists of four full-scale corner beam-column joint specimens with slabs. Two parameters were considered in the design of the beam cross sections to investigate the effects of joint aspect ratio and beam longitudinal reinforcement ratio. Column and slab cross section dimensions were identical for all four specimens but column longitudinal reinforcement ratios were changed to meet the strong column-weak beam scheme. The configuration of the specimens and their design details are summarized in Fig. 1. The material properties of specimen SP1 are presented in Table 1 where f_c' is the concrete compressive strength, and f_y and f_u are the reinforcing steel yield and ultimate strength. For the four specimens, the two orthogonal beam cross sections had different effective depth at the column face because the reinforcing bars of the East-West (EW) direction beam were placed under those of the North-South (NS) beam, as shown Fig. 2.

Sufficient shear reinforcements were provided in the beams and columns to avoid shear or torsional failures. All specimens were designed with eight bars in the column cross section, i.e. three bars per each side, Fig. 1. The details of beam reinforcement anchorage followed the minimum requirement of standard hook and the bottom reinforcement of slab extended six inches from the beam inner face, Figs. 1 and 2.

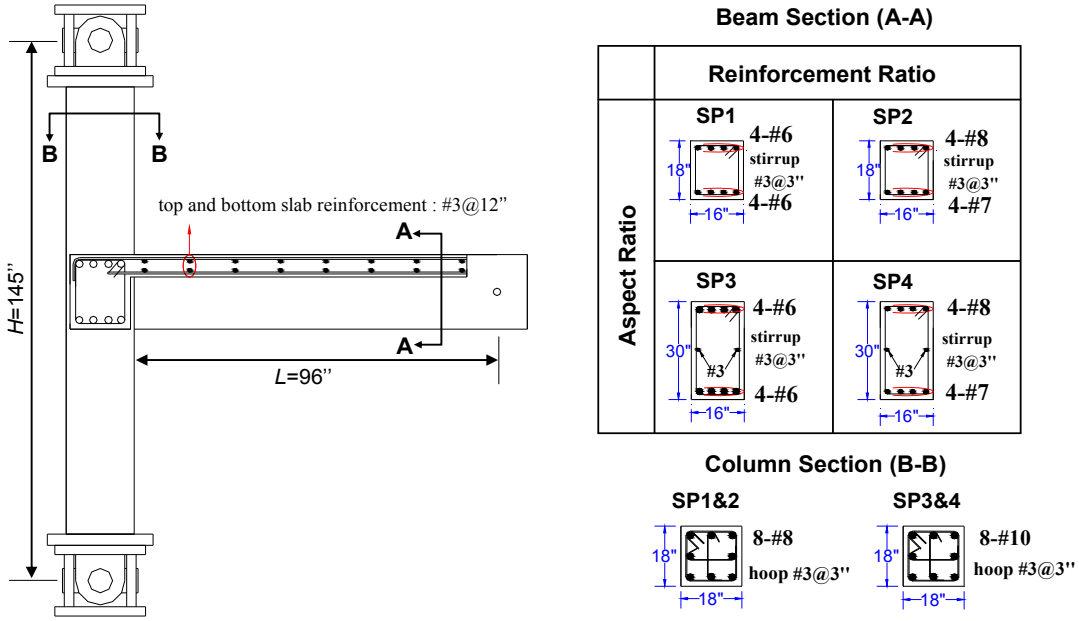

Figure 1. Configuration and design details of the specimens

Figure 2. Placement of beam reinforcements in specimen SP1.

Table 1. Material properties of specimen SP1.

Concrete	**Reinforcement**					
	#8 (25mm)		#6 (19mm)		#3 (10mm)	
f_c' (ksi)	f_y (ksi)	f_u (ksi)	f_y (ksi)	f_u (ksi)	f_y (ksi)	f_u (ksi)
3.71	72.2	103	78.6	105	73.5	115

Loading Protocol

The lateral load was applied in a quasi-static (0.02 in./sec) manner through displacement control at the end of each beam. The applied displacement alternated between the two directions of the beams, i.e. one beam remained at a reference point during the loading of the other orthogonal beam. Both beams were pulled down to one quarter of the estimated yield displacement (Δ_y=1.24 in. for specimen SP1) to simulate gravity load prior to the cyclic testing and this displacement was defined as the reference point (Δ_0). The number of peak displacement levels is limited to three values prior to yielding to reduce the unnecessary effect of low-cycle fatigue on the joint strength. Upon yielding, the peak displacement of the next level was determined as 1.5 times the previous displacement level. In the inelastic loading range, it is noted that single low-level cycle, being equal to 1/3 of the previous displacement level, was added after each group of cycles to quantify the stiffness degradation. The protocol of the displacement-controlled loading is depicted in Fig. 3.

The beam shear forces for the EW and NS directions, $V_{b,\mathrm{EW}}$ and $V_{b,\mathrm{NS}}$, respectively, corresponding to the applied displacements at each step were recorded in real time and these forces directly determined the applied column axial load by the following linear equations based on pre-test analyses of a selected prototype structure.

$$P_{\text{applied}} = -95 + 4V_{b,\mathrm{EW}} + 4V_{b,\mathrm{NS}} \quad \text{for specimens SP1 and SP2} \tag{1a}$$

$$P_{\text{applied}} = -95 + 2V_{b,\mathrm{EW}} + 2V_{b,\mathrm{NS}} \quad \text{for specimens SP3 and SP4} \tag{1b}$$

The determined column axial load was applied by two hydraulic actuators located on each side of column and constrained to apply the same axial displacement without rotation. It is noted that the column axial load varied linearly according to the applied beam shear forces from 83 kips in tension to 115 kips in compression during the test of SP1.

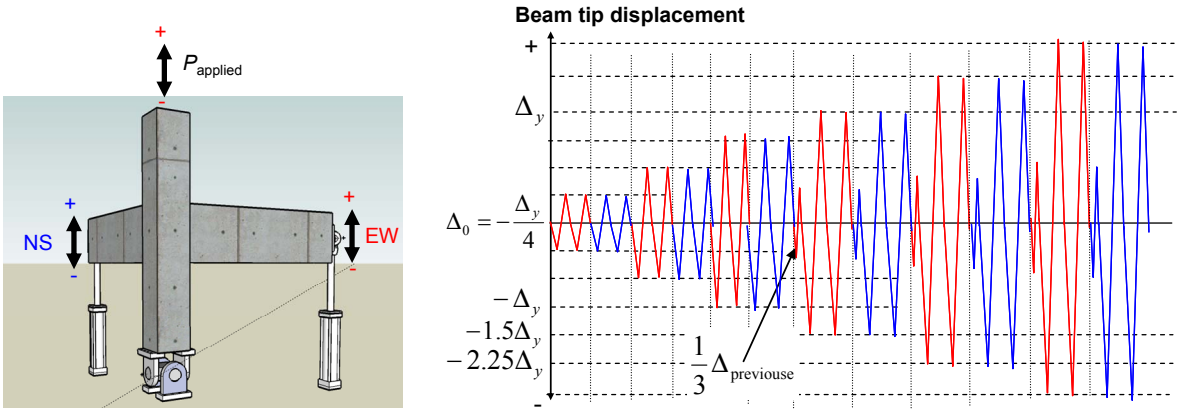

Figure 3. Displacement history.

Test Setup

The test setup consisted of a lateral restraining frame and two 3D clevises, Fig. 4. These clevises were introduced in such a way to achieve variable column axial loading and to satisfy the boundary conditions represented by inflection points in both directions (EW and NS) assumed to be located in the middle of both top and bottom columns and EW and NS beams of the prototype 3D building frame. Top and bottom ends of the column were artificially confined to prevent local failure during testing. In the test setup, no P-delta effect was taken into consideration.

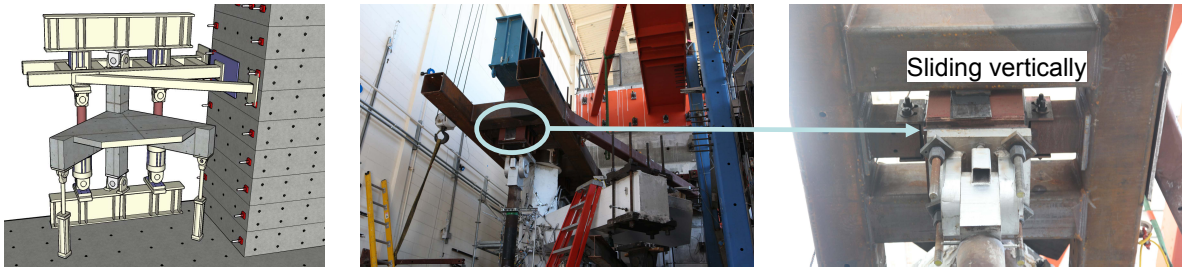

Figure 4. Test setup.

Experimental Results

The first test was conducted with specimen SP1 having low beam reinforcement ratio and low joint aspect ratio. The testing of the other three specimens is in progress. Specimen SP1 was designed to target joint shear failure following beam longitudinal reinforcement yielding in tension. The photographs and hysteresis plots of the beam shear versus drift showed that the failure of SP1 conformed to the intended failure in both directions (Fig. 5). It is noted that the drift is defined as the applied beam vertical displacement normalized by the length $L+0.5b_c$ where L is defined in Fig. 1 and b_c=18 in. is the column width, Fig. 1.

The joint rotation versus normalized joint shear stress is shown in Fig. 6. The joint rotation is approximated as the distortion angle due to the relative horizontal deformation between the top and bottom of the joint region, as shown by the inserts of Fig. 6. The joint shear stress is normalized by $\sqrt{f_c'}$, i.e. $V_{jh}/b_j h_c \sqrt{f_c'}$ where V_{jh} is the horizontal joint shear force, and b_j and h_c are the effective width of the joint (ACI 352-02) and column height in the direction of

loading, respectively. At the peak positive shear loads (i.e. upward), the positive joint rotations (i.e. slab in compression) in the two directions EW and NS were close and averaged about 0.01 rad. On the other hand, at the peak negative shear loads (i.e. downward), the negative joint rotations (i.e. slab in tension) in the two directions EW and NS were close and averaged about 0.005 rad.

The beam shear corresponding to nominal beam flexural yield strength without slab reinforcement contribution was estimated before the test to be 21 kips. The beam reinforcement yielding at applied beam shear forces in the range of 18.5 and 22.4 kips was confirmed by the data from the strain gages installed on the beam reinforcing bars (Fig. 7).

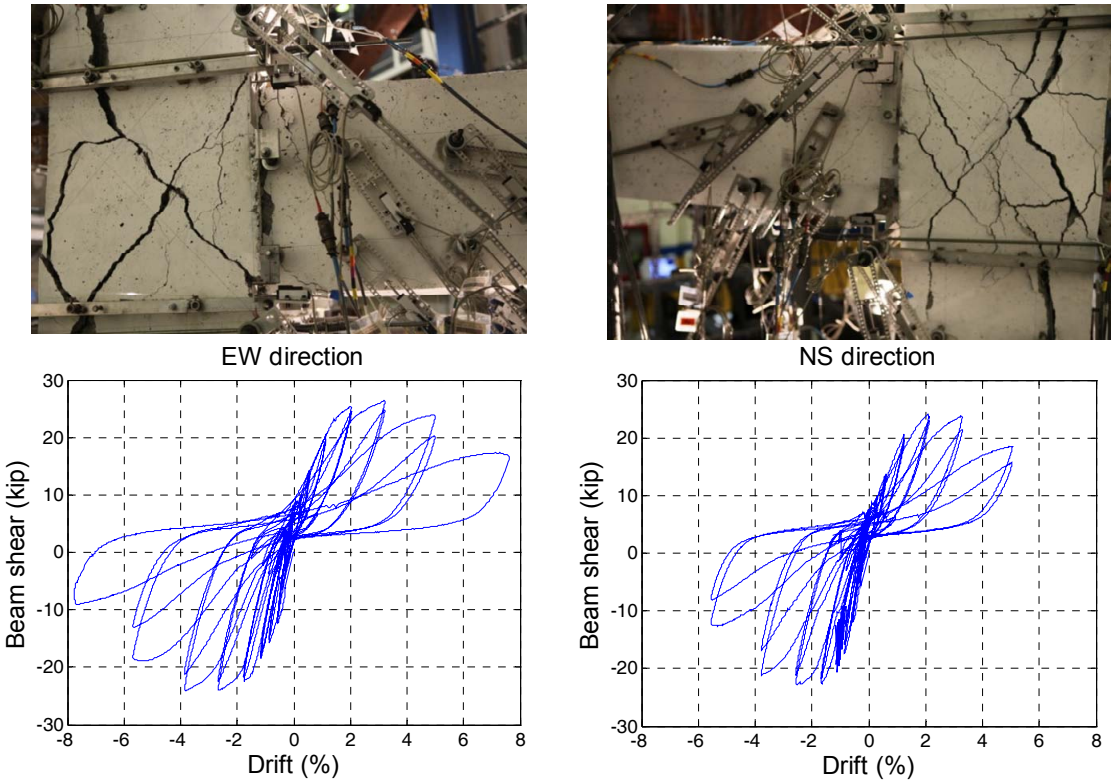

Figure 5. Beam shear-drift responses of SP1.

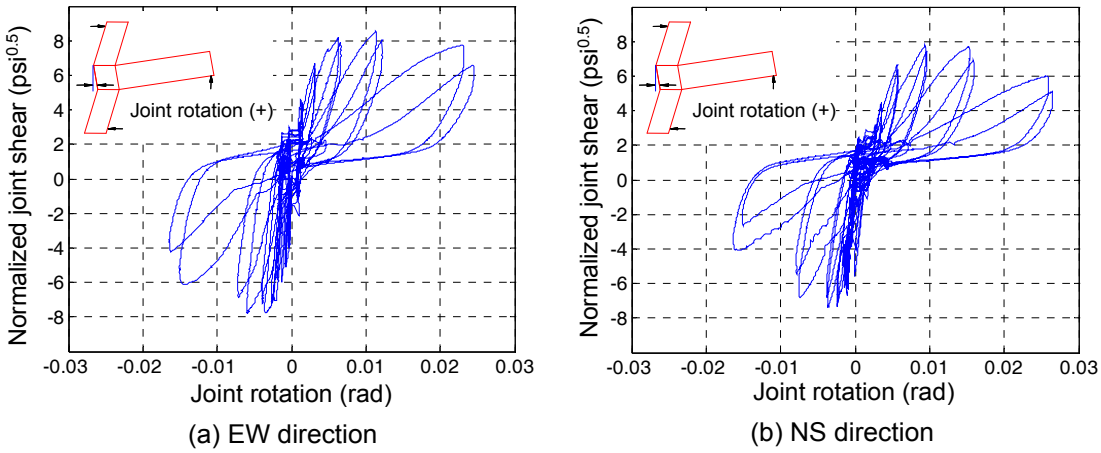

(a) EW direction (b) NS direction

Figure 6. Joint shear stress-rotation responses of SP1.

The reinforcements of the beams yielded at the column faces in both directions after loading of 1.2% drift which was analytically estimated as the yield drift. Fig. 7 shows that the beam reinforcement yielding propagated into the joint during continuous loading. It was also observed that the strain of the outer (external) beam top reinforcement, named "Top Ext.", was greater than that of the inner (internal) beam top reinforcement, named "Top Int.". Therefore, only results of the "Top Ext." bars are shown in Fig. 7.

The contribution of slab reinforcement to the horizontal joint shear stress is investigated by the strain distribution and crack propagation. The slab top reinforcement closest to column face yielded under the same loading when beam reinforcement yielded. At the peak level of loading (3.2% drift), three top reinforcing bars have yielded in the EW direction and two top reinforcing bars have yielded in the NS direction. It is clear that the slab bottom reinforcement contributed less than its top reinforcement in the joint response considering the anchorage details (Fig. 1), the ratio of beam depth (18 in.) to slab thickness (6 in.), and the observed slab cracks (Fig. 8). It was observed that flexural and torsional cracks took place in both beam and slab as shown in Fig. 8 and they were widely open at the peak loads. Torsional cracks in the slab circled from the column face with 12 in. diameter as shown in Fig. 8c. Based on these observations, it is concluded that the top slab reinforcing bars placed within beam depth from column face (top two #3 reinforcing bars in specimen SP1, refer to Fig. 1) participated in resisting the horizontal joint shear force.

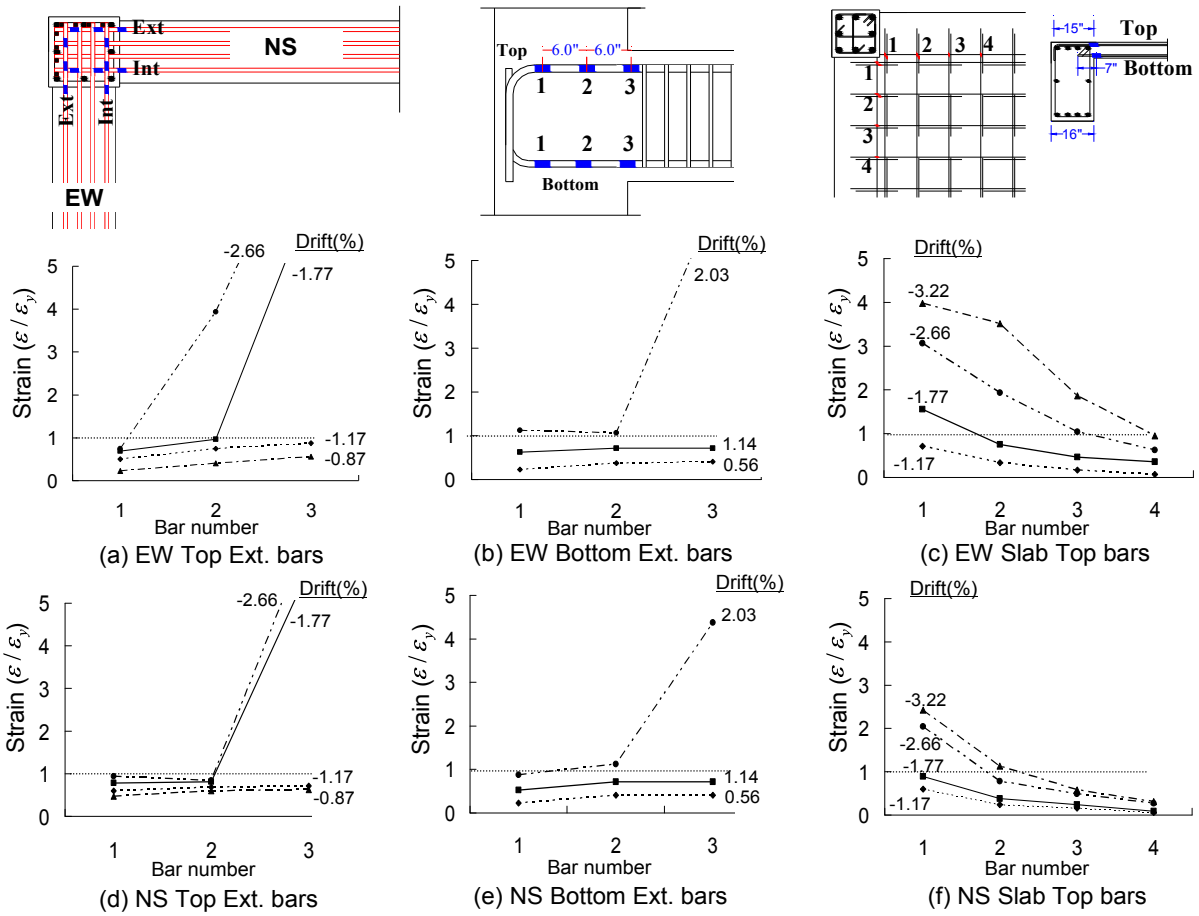

Figure 7. Measured strains at peak drifts of the beam and slab reinforcing bars of specimen SP1.

(a) EW side (b) NS side (c) Slab cracks

Figure 8. Joint shear failure of specimen SP1.

Analytical Prediction

Shear Strength Models

A large number of test data from literature were collected for unreinforced exterior joints without or with one lateral beam. Parametric study was performed with the constructed database and the shear strength models were proposed by semi-empirical and analytical approaches (Park and Mosalam 2009). The two joint shear strength models include the effect of joint aspect ratio and the amount of beam reinforcement on the joint shear strength. In this paper, these two models are briefly introduced and their shear strength predictions for specimen SP1 are compared with the test results. More details about the models can be found in (Park and Mosalam 2009).

Semi-Empirical Model

To develop a semi-empirical model, two basic concepts were assumed as follows: (1) maximum and minimum joint shear strengths are affected by the joint aspect ratio with no influence of the beam reinforcement index, and (2) joint shear strength is linearly proportional to beam reinforcement index between maximum and minimum joint shear strengths. It is noted that the beam reinforcement index is defined as the term in the square brackets of Eq. 2a. From these assumptions, the shear strength equation is proposed in [lb and in. units] as follows,

$$\frac{V_{jh}}{b_j h_c \sqrt{f_c'}} = \Phi\left[\left(\frac{A_s f_y}{b_j h_c \sqrt{f_c'}}\right)\left(1 - 0.85\frac{h_b}{H}\right)\right] \geq 10\frac{\cos\theta}{1.31 + 0.085\left(\frac{h_b}{h_c}\right)} \tag{2a}$$

$$\leq 23\frac{\cos\theta}{1.31 + 0.085\left(\frac{h_b}{h_c}\right)} \tag{2b}$$

where A_s and f_y are the total cross section area and yield strength of beam reinforcement in tension, respectively, h_b is the height of the beam cross section, H is the height between upper and lower column inflection points, $\theta = \tan^{-1}(h_b/h_c)$, and Φ is the over-strength factor due to strain hardening of the beam reinforcement. For simplicity, Φ is assumed to be 1.25 at the minimum joint shear strength and decreases linearly to $\Phi = 1.0$ at the maximum joint shear strength.

Analytical Model

In the analytical model, two inclined struts were assumed to resist the horizontal joint shear in a parallel system (Fig. 9). The major diagonal strut (ST1) is developed by the diagonal compression, while the minor inclined strut (ST2) is developed by the bond resistance of the concrete surrounding the beam reinforcement.

The horizontal joint shear force is approximated from the global equilibrium of a joint panel and decomposed as follows,

$$V_{jh} = V_{jh,ST1} + V_{jh,ST2} = A_s f_s - V_c \approx A_s f_s \left(1 - 0.85\frac{h_b}{H}\right) \tag{3a}$$

$$V_{jh,ST1} = A_s f_s - n\pi\phi_b \int_0^{l_h} \mu(f_s)dx \tag{3b}$$

$$V_{jh,ST2} = n\pi\phi_b \int_0^{l_h} \mu(f_s)dx - V_c \tag{3c}$$

where V_c is the shear force in the column, n is the number of beam longitudinal reinforcement in tension with diameter ϕ_b, $l_h = h_c - a_c$ is the horizontal projection of ST2 with a_c defined in Fig. 9 and in (Park and Mosalam 2009), and $\mu(f_s)$ is the bond stress distribution along the beam reinforcement as a function of the tensile stress f_s, which varies with the coordinate x along the bar, i.e. $f_s = f_s(x)$. To relate each strut equilibrium equation to the total horizontal joint shear force, a fraction factor is introduced to determine the contribution of ST1, i.e. $V_{jh,ST1} = \alpha V_{jh}$ and the expression of this fraction factor is determined as follows,

$$A_s f_s - n\pi\phi_b \int_0^{l_h} \mu(f_s)dx = \alpha A_s f_s \left(1 - 0.85\frac{h_b}{H}\right) \Rightarrow \alpha = \frac{H}{H - 0.85h_b}\left(1 - \frac{4}{\phi_b}\frac{\int_0^{l_h}\mu(f_s)dx}{f_s}\right) \tag{4}$$

The fraction factor is simplified as tri-linear curve and the breaking points are derived as follows,

$$f_o = \frac{4}{\phi_b}\mu_E l_h, \quad f_p = f_y + \frac{4}{\phi_b}\mu_Y l_h, \quad f_r = \frac{4}{\phi_b}\frac{H}{0.85h_b}\int_0^{l_h}\mu(f_r)dx \geq f_p \tag{5a}$$

$$\alpha_1 = \frac{H}{H - 0.85h_b}\left(1 - \frac{4}{\phi_b}\frac{\mu_E}{f_y}l_h\right), \quad \alpha_2 = \frac{H}{H - 0.85h_b}\left(1 - \frac{4}{\phi_b}\frac{\mu_Y}{f_y + \frac{4}{\phi_b}\mu_Y l_h}l_h\right) \leq 1.0 \tag{5b}$$

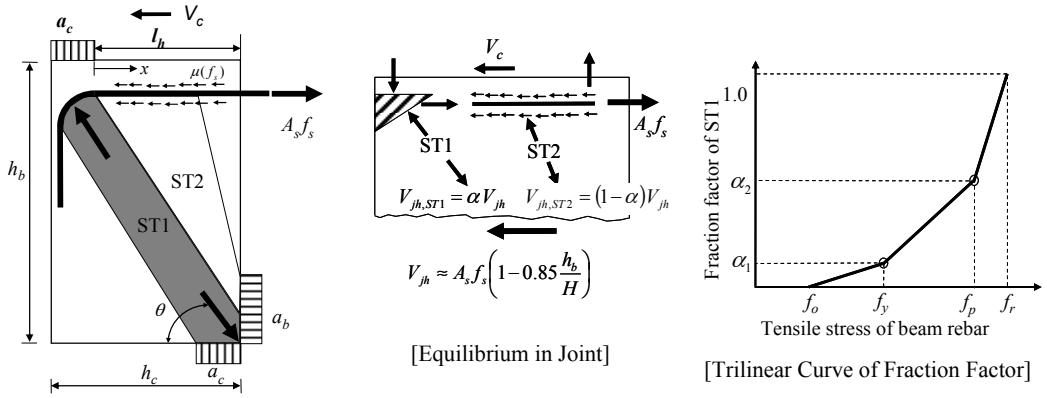

[Equilibrium in Joint] [Trilinear Curve of Fraction Factor]

Figure 9. Assumed mechanism and fraction factor.

where $\mu_E = 12\sqrt{f_c'}$, $\mu_Y = 0.5\mu_E$, and $\mu_r = 0.15\mu_E$ (Park and Mosalam 2009). It is noted that the tensile stress f_r in Eq. 5a is obtained implicitly by letting $\alpha = 1.0$ in Eq. 4 since the bond distribution cannot be explicitly defined at $\alpha = 1.0$. The beam-column joint shear strength is defined when the demand of ST1 reaches its capacity obtained from

$$V_{jh,ST1,\max} = 8.3 \frac{b_j h_c \sqrt{f_c'} \cos\theta}{1.31 + 0.085\left(\frac{h_b}{h_c}\right)} \tag{6}$$

Considering the fraction factor relationship in Fig. 9, and the capacity of ST1 from Eq. 6, the joint shear strength is calculated by an iterative procedure using the algorithm illustrated in Fig. 10.

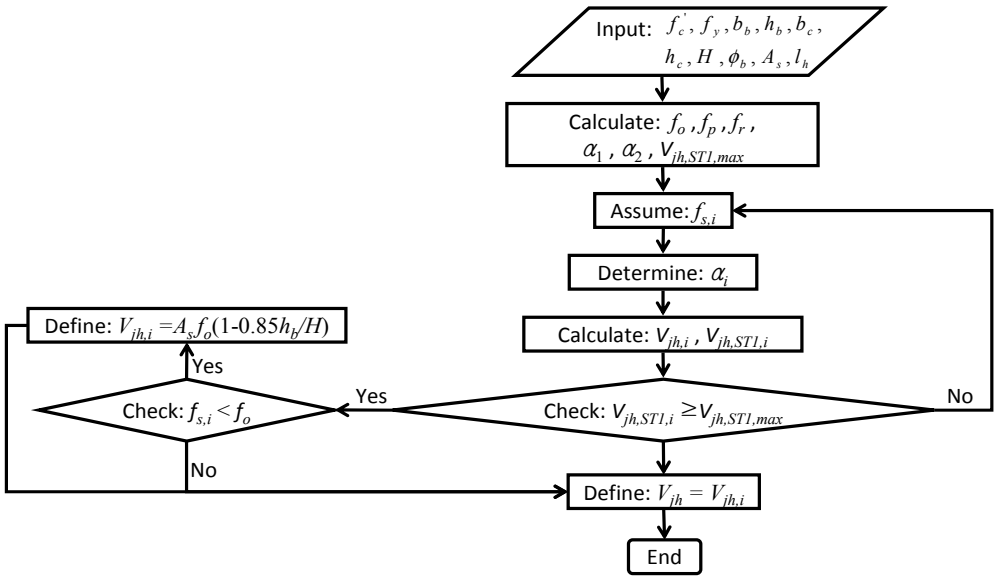

Figure 10. Solution algorithm of the proposed analytical model.

Prediction of shear strength

The joint shear strength of specimen SP1 is predicted by the aforementioned two models and compared with the test results. The horizontal joint shear force from the test is calculated using the recorded beam shear with constant moment arm assumption, i.e. $jd = 0.9d_b$, where d_b is the effective depth of the beams, refer to Fig. 2 and Table 2. The contribution of slab

Table 2. Comparison of the joint shear strength, $V_{jh}/b_j h_c \sqrt{f_c'}$, predictions with test result.

Loading		d_b (in.)	Test (psi$^{0.5}$)	Semi-empirical (psi$^{0.5}$)	Analytical (psi$^{0.5}$)
EW	Up (+)	16.125	8.3	7.7 (0.93)*	7.6 (0.92)*
	Down (-)	14.764†	8.4	8.4 (1.00)*	8.3 (0.99)*
NS	Up (+)	15.625	7.9	7.7 (0.97)*	7.6 (0.96)*
	Down (-)	15.153†	7.8	8.4 (1.08)*	8.3 (1.06)*

*( ) the ratio of the joint shear strength prediction to the test result

†effective depth includes contribution of top 2-#3 slab reinforcement

reinforcement is considered by adding the effect of two of the top reinforcing bars (2-#3) in the joint shear calculation for downward loading. The predictions by both semi-empirical and analytical models show reasonable accuracy (within +8% and -7% for the semi-empirical model and within +6% and -8% for the analytical model) as shown in Table 2.

Conclusions

The purpose of testing specimen SP1 is to investigate the joint shear strength of unreinforced corner beam-column joint with low beam reinforcement ratio (0.67%) for a case with low joint aspect ratio (1:1). Moreover, the paper presented two models for determining the joint shear strength using semi-empirical and analytical approaches. From the results of the test and the analytical predictions using the developed models, the following conclusions can be made:

1. The failure of specimen SP1 was governed by joint shear following beam yielding as intended in its design. The joint shear strength is determined to be $8.1 b_j h_c \sqrt{f_c'}$ [lb and in. units] on average. This joint shear strength is greater than that of unreinforced (nonconforming transverse reinforcement) exterior joint from ASCE/SEI 41-06, i.e. $6 b_j h_c \sqrt{f_c'}$ [lb and in. units].

2. Considering the contribution of the slab reinforcement in specimen SP1, the slab top reinforcing bars placed within the beam depth from the column face appeared to have participation in the joint shear strength. In other words, the slab contribution to the load input into the beam-column joint can be estimated by considering the effective slab width as the beam depth from the column face for the case of beam yielding followed by joint shear failure.

3. The newly developed joint shear strength models using semi-empirical and analytical approaches include the effect of joint aspect ratio and the amount of beam reinforcement on the joint shear strength. These two models accurately (with≤8% error) predicted the joint shear strength of specimen SP1 which failed in joint shear following beam yielding.

Acknowledgments

This study is supported by the NSF award #0618804 through PEER, University of California, Berkeley. NSF financial support is gratefully acknowledged. Opinions, findings or recommendations expressed in this paper are those of the authors and do not necessarily reflect those of NSF. The authors acknowledge the technical contribution of Prof. J.P. Moehle and Mr. W. Hassan. The laboratory assistance of nees@berkeley staff was essential for the experimental part of the study.

References

ACI Committee 352, 2002. *Recommendation for Design of Beam-Column Connections in Monolithic Reinforced Concrete Structures* (ACI-352-02), American Concrete Institute, Farmington Hills, Mich.

ASCE/SEI Seismic Rehabilitation Standards Committee, 2007. *Seismic Rehabilitation of Existing Buildings* (ASCE/SEI 41-06), American Society of Civil Engineers, Reston, VA.

Park, S., and Mosalam, K.M., 2009. Shear Strength Models of Exterior Beam-Column Joints without Transverse Reinforcement, *PEER Report 2009/106,* University of California, Berkeley.